# From microhardness to fatigue life: a review of predictive approaches for surface-hardened mechanical components

Marco V. Boniardi, Edoardo Scabini, Andrea Casaroli
*Department of Mechanical Engineering, Politecnico di Milano, via La Masa 1, 20156 Milano, Italy*
*marco.boniardi@polimi.it , https://orcid.org/0000-0002-2438-7890*
*edoardo.scabini@polimi.it , https://orcid.org/0009-0005-4487-912X*
*andrea.casaroli@polimi.it , https://orcid.org/0000-0001-5207-5547*



**ABSTRACT.** This review paper aims to systematically examine the effects that the most common thermal and thermochemical surface hardening treatments - specifically surface hardening, carburising, and nitriding - have on the fatigue strength of mechanical components, which has historically been the primary cause of failure during service.
Following a brief description of the heat treatments and the mechanical and metallurgical effects they produce on components, a predictive model of the fatigue strength of surface-hardened mechanical components subjected to bending stresses is presented, using the local fatigue limit approach.
The parameters used in the model are the microhardness profile of the hardened zone, the distribution of residual stresses in the hardened layer, the fatigue strength of the base material, and the stress state induced by external forces. The proposed model was validated for three real-world cases: surface hardened specimen with a notch, smooth carburised specimen and smooth nitrided specimen. The results provide important insights from both an academic and industrial perspective. In fact, they allow for the determination of which parameters must be controlled to increase the fatigue strength of surface-treated mechanical components.

**KEYWORDS.** Surface hardening, Carburising, Nitriding, Fatigue strength, Microstructure, Microhardness, Residual stresses, Local fatigue limit.

OPEN ACCESS

**Citation:** Boniardi, M. V., Scabini, E., Casaroli, A., From microhardness to fatigue life: a review of predictive approaches for surface-hardened mechanical components, Fracture and Structural Integrity, 77 (2026) 405-420.

**Received:** 11.05.2026
**Accepted:** 08.06.2026
**Published:** 14.06.2026
**Issue:** 07.2026

## INTRODUCTION

Surface treatments, both thermal (surface hardening) and thermochemical (carburising and nitriding), are performed on many components produced with different technological processes [1–3] to improve their mechanical properties, particularly wear resistance. It is well known that these heat treatments increase the surface hardness of the steel and, consequently, improve the wear resistance of the component itself [4–8]. In the case of surface hardening [7,9], the increase in hardness is due to the hardening treatment (induction, laser, or flame) performed exclusively on the surface of the component, after it has been quenched and tempered throughout its cross-section. At the end of the process, the component has both good strength and toughness at the core (thanks to the quenching followed by tempering), and simultaneously exhibits high surface hardness (resulting from the surface hardening followed by stress relief). This is also why medium- to high-carbon steels (42CrMo4, C45) are preferred for surface hardening. The situation is different, however, during the thermochemical processes of carburising and nitriding: in addition to a thermal effect, in both cases a chemical reaction occurs between the process atmosphere and the carbon or low-alloy steel. Carburising [9,10], which is typically performed on low-carbon steels (C ≤ 0.2%) using hydrocarbon gas atmospheres (methane, propane, etc.), results in increased hardness due to the carbon enrichment of the steel's surface: subsequent quenching produces a carbon-rich martensitic structure on the surface (approximately C = 0.8%) along with a carbon-poor martensitic structure in the core (C ≤ 0.2%). In metallurgy, this is commonly referred to as hardening due to the interstitial solid solution of carbon in the iron lattice. Finally, nitriding [9]: this process is typically carried out in an ammonia atmosphere and is applied to medium-carbon steels that are lightly alloyed with chromium, molybdenum, and, in some cases, aluminium and vanadium. By enriching the surface of a steel workpiece with nitrogen, it is possible to induce the formation of nitrogen phases with iron and other alloying elements (ε and γ' phases): the presence of these phases, in the form of small particles finely dispersed in the surface layer, locally deforms the original α-iron lattice, producing a significant increase in the steel's hardness. In metallurgy, this is commonly referred to as precipitation hardening.

In all three cases discussed, we are dealing with thermal or thermochemical processes that induce an increase in the surface hardness of the heat treated steel components. Fig. 1 shows a schematic representation of the hardness profiles produced by the three surface heat treatments already described. Note how the three surface heat treatments are complementary to one another in terms of both maximum hardness and effective depth.

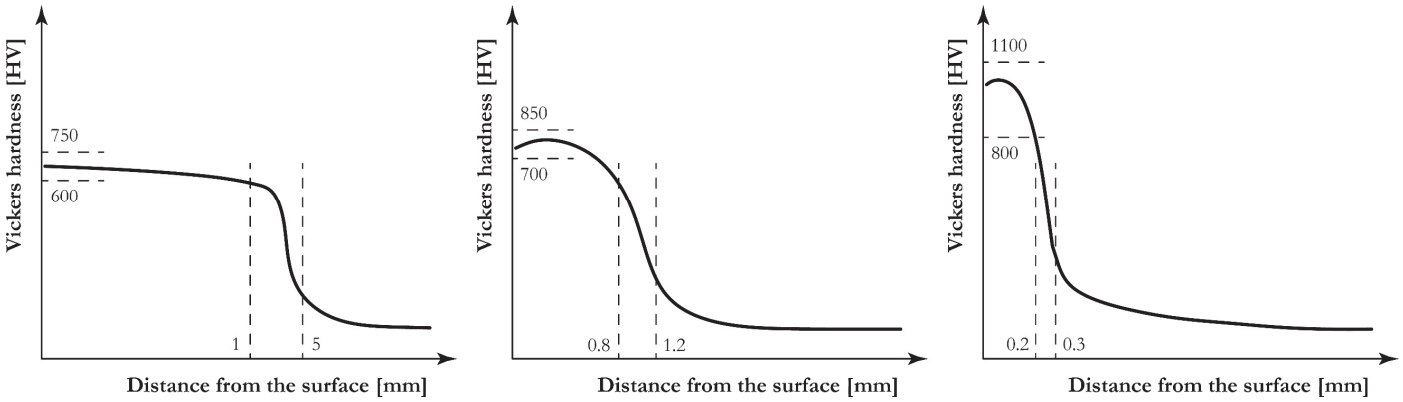


Figure 1: Schematic representation of hardness profiles for a component that is (left) surface-hardened, (center) carburised and (right) nitrided. The values represent the typical maximum hardness and effective depth for the three surface treatments.

There is an additional effect caused by the three hardening processes already described: in addition to the hardness increase, a residual compressive stress affects the whole hardened zone. These residual compressive stresses are always a direct consequence of the process that led to the surface hardening [11,12].

In the case of surface hardening, the effect is a direct consequence of the increase in specific volume induced by the austenite-martensite transformation. In the surface area (where the steel hardens), the specific volume change is effectively prevented by the underlying layers of material (which do not undergo the surface heat treatment): the consequence is the formation of residual compressive stresses, balanced by residual tensile stresses in the core.

As for carburising, the situation is slightly more complex, although the final effect can always be attributed to the increase in specific volume resulting from the austenite-martensite transformation. During the quenching process (i.e., after carburisation, when the surface has already been enriched with carbon), on small and medium-sized parts, the austenite-

martensite transformation of the core will be observed first, followed by that of the surface. This generates residual compressive stresses on the surface and tensile stresses in the core, exactly the opposite of what occurs during conventional quenching. Finally, in the case of nitriding, the internal stresses arise from the formation of nitrogen-rich phases which, by distorting the crystal lattice, develop residual compressive stresses in the area where the nitrogen concentration is higher than that of the base metal (i.e., throughout the area subject to nitrogen diffusion).
Fig. 2 shows the distribution of residual axial stresses in a cylindrical specimen subjected to each of the three surface treatments described. Note that, in the case of surface hardening, the maximum residual stress occurs at the surface, whereas for carburied and nitrided layers, the highest residual stresses develop below the surface.

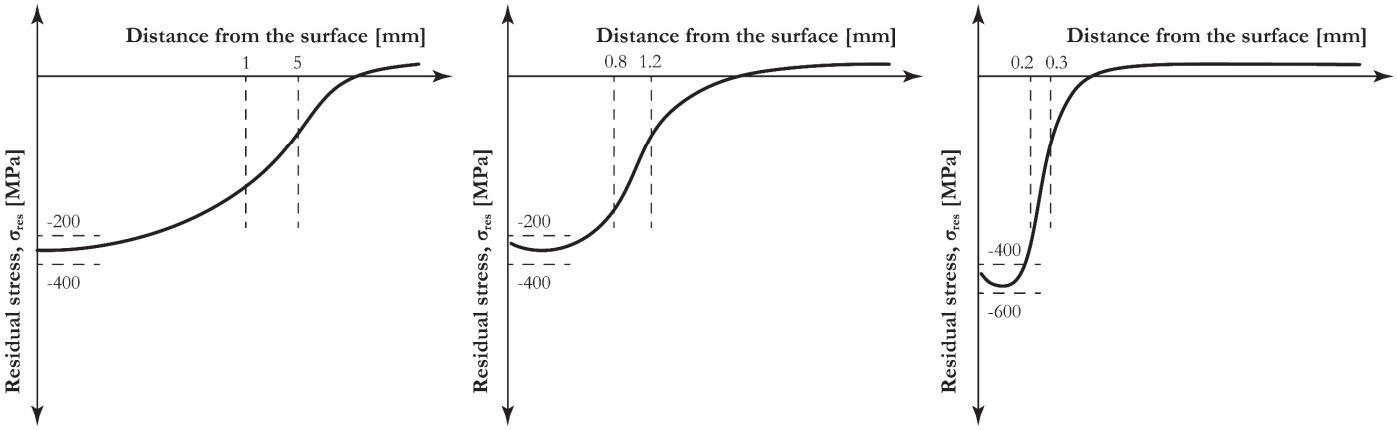


Figure 2: Schematic representation of residual stresses in a component subjected to surface hardening treatment: (left) surface-hardened, (center) carburised and (right) nitrided.

## THE STRESS STATE INDUCED BY EXTERNAL FORCES

Before examining in detail the effect of surface treatments on the fatigue strength of mechanical components, let us consider the stress states that occur in components due to external forces. Let us consider a basic loading condition and a component with a simple geometry: bending applied to a cylindrical shaft. It is well known in mechanical engineering [4,13] that the nominal stress state ($\sigma_{0,r}$) induced in a smooth cylindrical component of diameter, $d$, due to bending $M_f$, is a function of the moment of inertia $I$ and the radial position, $r$, and is given by:

$$\sigma_{0,r} = \frac{M_f}{I} r = \frac{M_f}{\pi d^4 / 64} r \tag{1}$$

$$\sigma_{0,\,sup} = \frac{M_f}{\pi d^4 / 64} \cdot d/2 = \frac{M_f}{\pi d^3 / 32} \tag{1bis}$$

The value of $\sigma_{0,r}$ (1) reaches its maximum on the outer surface of the cylinder, $\sigma_{0,sup}$ (1bis), and decreases linearly with the radius $r$ until it becomes zero on the axis of the cylinder (Fig. 3a).
If the component were notched, i.e. if it had a change in cross-section or any geometric discontinuity, a local effect of stress concentration would be observed.
To evaluate this local effect of increased stresses (notch effect), it is usual to introduce a geometric stress concentration factor $K_t$ which provides the value of the maximum surface stress according to the relationship:

$$\sigma_{max} = K_t \cdot \sigma_{0,sup} \tag{2}$$

In this case, however, the surface stress given by Eqn. (2) does not decrease linearly with the radius, but instead exhibits a rather steep gradient. This effect occurs because, when the same bending is applied to both the smooth and the notched shafts, the integral of the stress distribution across the cross-sections of the two shafts must remain constant (Fig. 3b).

The stress concentration factor $K_t$ depends on the cross-sectional geometry and, in the specific case shown in Fig. 3b, on: (i) the fillet radius, (ii) the maximum and (iii) minimum diameters of the shaft; $K_t$ is normally tabulated for the most common notch shapes used in mechanical design (Fig. 4).

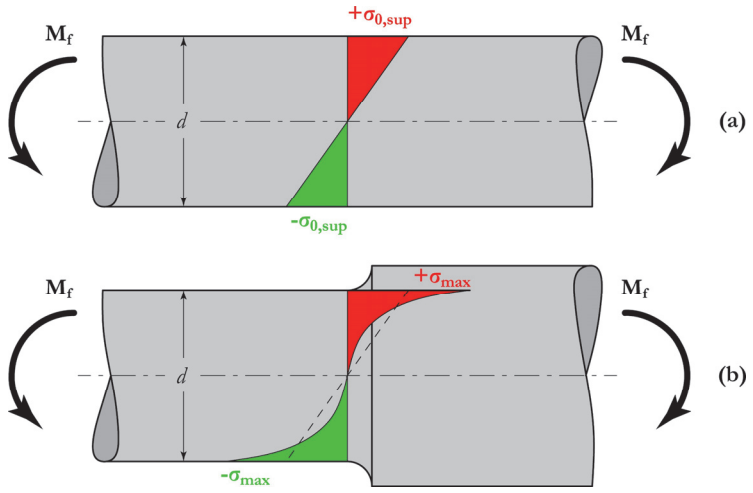


Figure 3: Stress distribution generated by bending applied to (a) a smooth shaft and (b) a notched shaft.

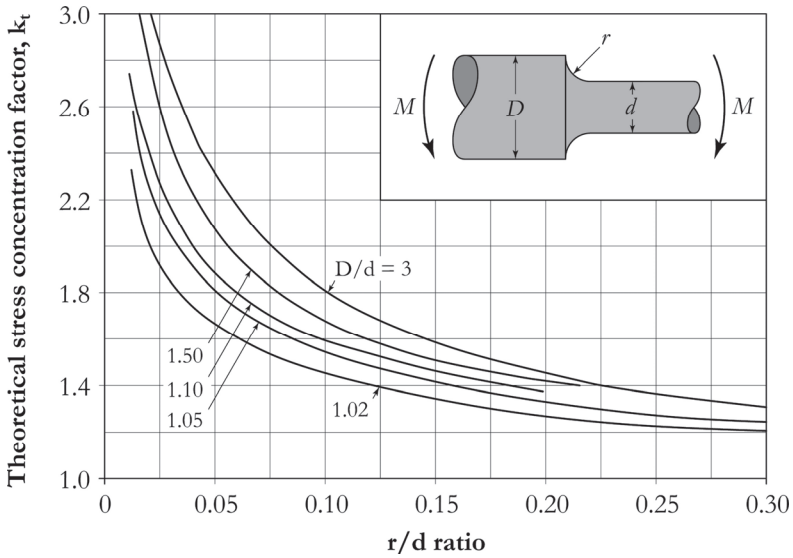


Figure 4: Stress concentration factor $K_t$ for a shaft with a shoulder subjected to bending [14].

Although the value of $K_t$ can only be applied to the surface of the component, i.e. near the notch, there are equations which, for various specific cases, allow the stress gradient caused by the notch to be calculated. In the case of bending condition shown in Fig. 3b, Nakonieczny [15] proposed the following equation to evaluate the maximum stress ($\sigma_{r,max}$) at every position along the section due to the stress gradient:

$$\sigma_{r,max} = K_t \, \sigma_{0,sup} [1 - \left( 2r / d \right)]^{3K_t - 2} \tag{3}$$

where $K_t$ is the stress concentration factor, $\sigma_{0,sup}$ is the nominal surface stress, calculated using Eqn. (1bis), and $r$ and $d$ are the radial position and the diameter of the cylindrical section, respectively.
Using (1), (1bis), (2) and (3), it is therefore possible to calculate the stress state at every point along a cylindrical section, whether smooth or notched, under the effect of bending.
Fig. 5 shows an application of (3) for a cylindrical section ($d$ = 6 mm) subjected to bending, with a maximum nominal stress of 100 MPa and different values of $K_t$.

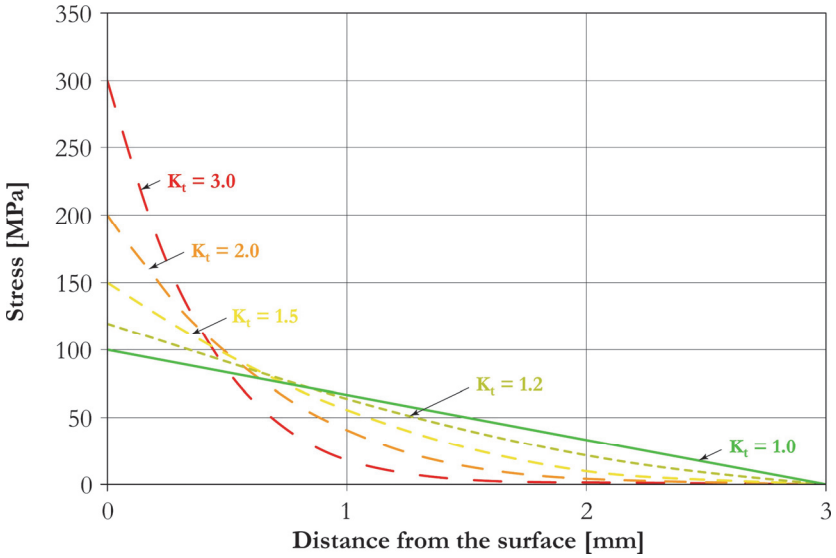


Figure 5: Stress analysis along a cylindrical section ($d$ = 6 mm) subjected to bending, as a function of different values of $K_t$ (maximum nominal stress 100 MPa).

## SURFACE TREATMENTS AND FATIGUE RESISTANCE

Having examined the stress state generated in mechanical components as a result of applied external forces, it is now possible to assess how the fatigue strength of these components can be improved through surface treatments. Although surface hardening, carburising and nitriding treatments are primarily carried out with the aim of increasing the wear resistance of steels, there is also another important advantage associated with these hardening processes: the systematic improvement of the steel's fatigue resistance, particularly in the field of high-cycle fatigue resistance [16,17]. The mechanism of the fatigue phenomenon involves the initiation and propagation of a crack that develops along the component section due to the cyclic stresses during operation. The engineering description is still the one proposed by Wöhler at the end of the 19th century and refers to the classic 'stress-cycle' diagram (S-N curve or Wöhler curve). Below a certain stress threshold (known as the fatigue limit $\sigma_{FA}$), neither component failure nor the propagation of fatigue cracks will occur, regardless of the number of cycles of the applied load. See in this regard the case illustrated in Fig. 6, which refers to the S-N curves for a quenched and tempered Cr-Mo steel and a quenched, tempered and nitrided Cr-Mo steel [14].

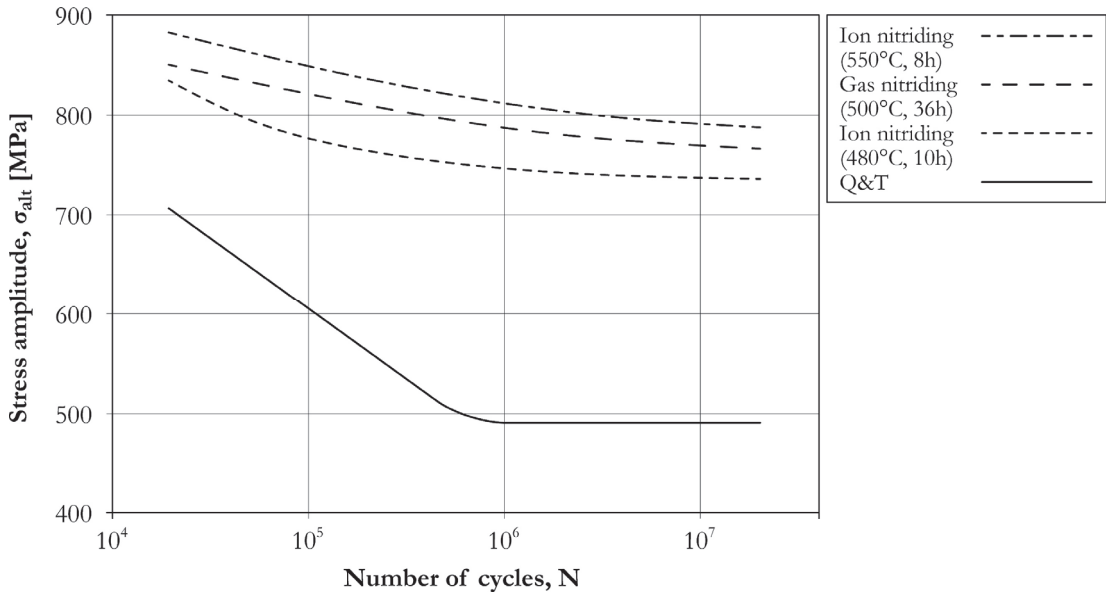


Figure 6: S-N diagram ($R = \sigma_{min}/\sigma_{max}$ = -1) for a chromium-molybdenum steel (AISI/SAE 4140 grade, similar to 42CrMo4), subjected to quenching and tempering and to quenching, tempering and nitriding using different processes [14].

As already noted, a fatigue crack initiates and propagates as a result of the normal loads applied during service: in high-cycle fatigue conditions, these loads are generally lower than those required to induce permanent plastic deformation of the component. However, due to surface irregularities or microstructural discontinuities, local stresses exceed the yield strength; consequently, when the load is applied cyclically, local plastic deformation develops.

The initiation and propagation of a fatigue crack are, therefore, the result of the simultaneous action of repeated cyclic stresses, tensile stresses and the resulting local plastic deformation. In the absence of even one of these three conditions, the nucleation and growth of a fatigue crack cannot occur. Cyclic stress allows the crack to form, whilst the tensile component of the applied stress allows it to propagate; the compressive component of the stress is irrelevant as it simply tends to close the crack tip without causing any damage [18].

This brief overview of the phenomenon of fatigue make it possible to identify two approaches for reducing or preventing both the damage nucleation and subsequent propagation:

1. increasing the mechanical strength of the steel through strengthening mechanisms that limit local plastic deformation;
2. generate residual compressive stresses that counteract external stresses, reducing the tensile load.

Surface hardening, carburising and nitriding heat treatments perfectly meet these two requirements: if the steel is selected appropriately and the treatment is carried out correctly, a significant increase in surface mechanical strength will be observed, as well as the development of compressive stress states in the surface layer. These two results produce a dual benefit in terms of fatigue behaviour:

- the improvement in the mechanical strength of the heat treated layer (measured as an increase in hardness) locally confers a higher fatigue resistance, $\sigma'_{FA}$, to the workpiece (Fig. 7). The linear correlation, valid for most steels, between fatigue limit and tensile strength is well known (Fig. 8) [14,16,19]: as hardness increases, in fact, the mobility of dislocations that could trigger fatigue is reduced.

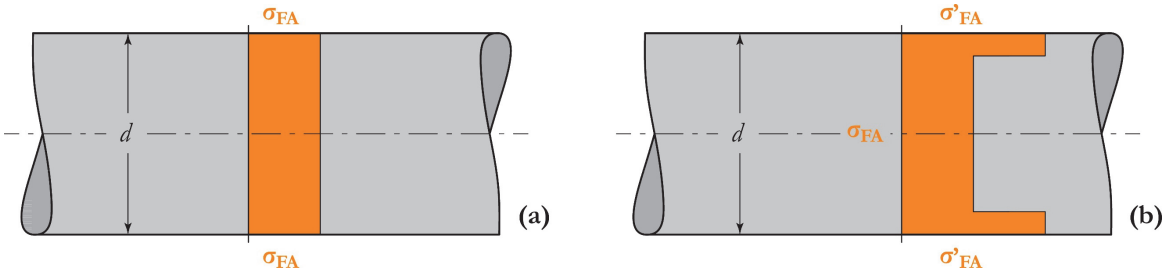


Figure 7: Fatigue limit for a component (a) with uniform fatigue strength, (b) with surface heat treatment ($\sigma_{FA}$: fatigue limit of the base material; $\sigma'_{FA}$: fatigue limit of the hardened surface layer).

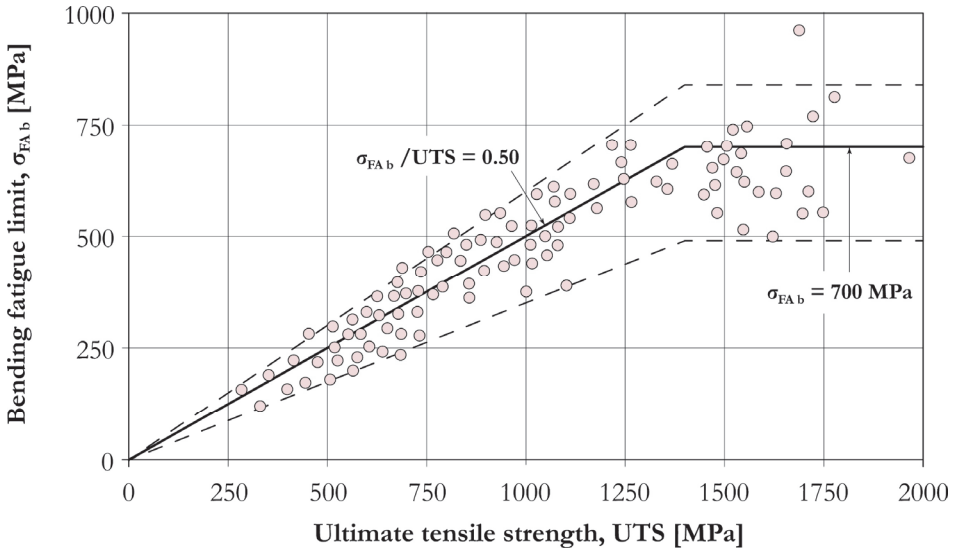


Figure 8: Correlation between ultimate tensile strength (UTS) and bending fatigue limit ($\sigma_{FAb}$). Note that, at least up to 1400 MPa, the bending fatigue limit (R = -1) is usually between 0.45 and 0.5 of UTS [14].

- Compressive residual stresses at the surface, balanced by limited tensile residual stresses in the core, significantly alter the distribution of applied external stresses. In this regard, consider the scheme in Fig. 9, which refers to a smooth

cylindrical piece subjected to bending. Fig. 9a shows the distribution of residual stresses induced by the surface heat treatment, while Fig. 9b shows the trend of the stresses induced by the applied bending; Fig. 9c shows the two superimposed stresses, and Fig. 9d their algebraic sum [20].

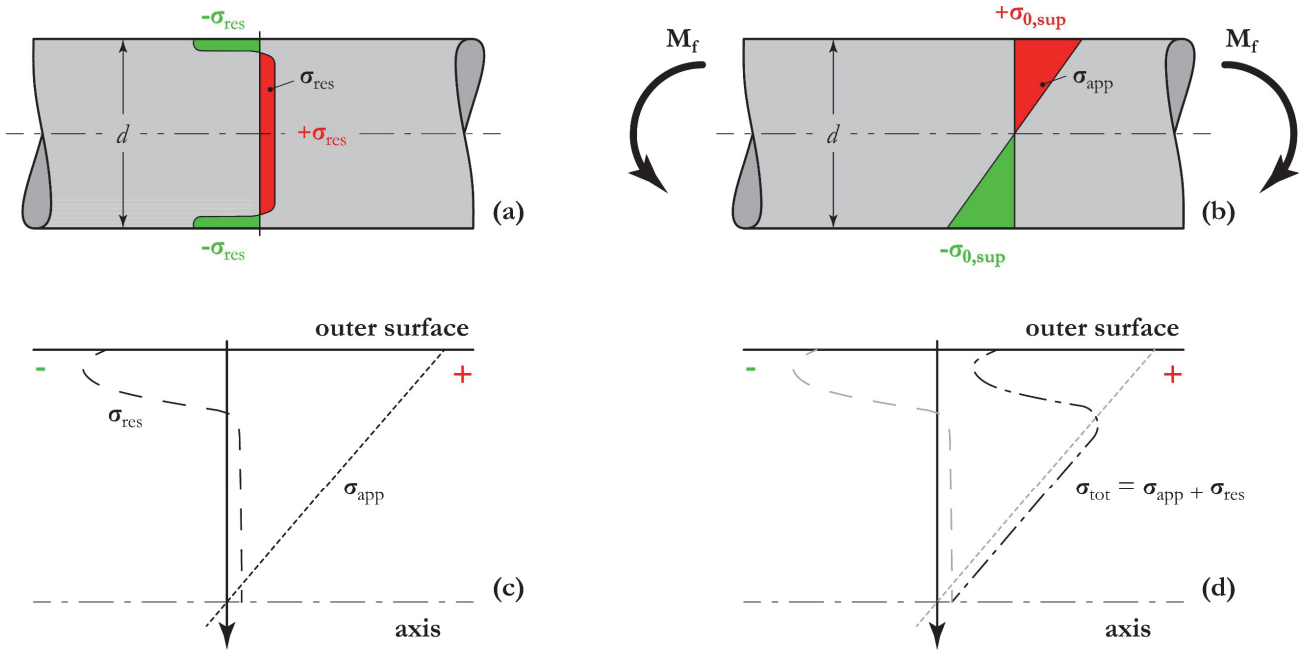


Figure 9: Stress states present in a cylindrical component: (a) due to a surface hardening heat treatment, (b) due to an applied bending, (c) superposition of the two stress states and (d) algebraic sum of the two stress states.

The comparative analysis of Fig. 7 and Fig. 9 also highlights another important aspect: the increase in fatigue resistance of a mechanical component is maximum when the applied external stresses are induced by bending or torsional loads (i.e. the applied stresses are maximum on the surface and decrease moving towards the axis). In the case of axial loads, however, the uniform distribution of stresses along the cross-section does not allow surface heat treatments to induce a significant improvement in fatigue behaviour. Tab. 1 reports the results obtained on nitrided cylindrical specimens, stressed according to different loading modes [16].

| Heat treatment | Bending fatigue limit [MPa] | Torsion fatigue limit [MPa] | Axial fatigue limit [MPa] |
|---|---|---|---|
| Quenching & Tempering | 565 | 315 | 540 |
| Quenching & Tempering + Nitriding | 750 | 410 | 540 |

Table 1: Fatigue limit of a steel in the quenched and tempered condition (UTS = 1150 MPa) and in the quenched, tempered and nitrided condition, subjected to cyclic bending, torsion and axial loads.

After defining the general aspects, we will now examine each hardening treatment in detail (surface hardening, carburising and nitriding), highlighting the main aspects in relation to the fatigue resistance of mechanical components.

### *Surface hardening*

Surface hardening (flame, induction, or laser) is a widely used surface hardening heat treatment for various types of mechanical components (shafts, axles, gears, etc.): the first applications of this treatment date back to the decade before World War II and concerned crankshafts [21]. From a metallurgical perspective, the aspects to consider in relation to the fatigue problem of surface-hardened components are listed below.

a. For surface hardening to be successful, the carbon present in the steel, in solution or in the form of carbides, must be distributed homogeneously and uniformly throughout the crystal lattice during the austenitization phase. However, the high speed of the heating phase (< 10 seconds), typical of surface hardening treatments, makes the diffusion of carbon into the metal matrix very difficult.

Consequently, at the end of the heat treatment, non-uniform or limited surface hardness may occur if the steel initially presents a coarse-grained ferritic-pearlitic structure, in which the pearlite is richer in carbon than the ferrite. For this reason, it is always better to surface-harden martensite in which the carbon is more homogeneously and uniformly distributed in the crystal lattice [21].

b. Great care must be taken to ensure a uniform hardening depth along the profile of the part. In addition to ensuring homogeneous strength, this result also allows for a uniform distribution of compressive residual stresses in the hardened surface layer, with beneficial effects on the fatigue resistance of the component [9,22].

c. If the treatment is performed correctly and the residual stresses on the surface are compressive, the fatigue fracture of an induction-hardened component shows initiation beneath the quenched layer. See two typical examples in Fig. 10. This morphology is valid for smooth parts or parts with limited notch effects; as the notch effect increases, the initiation will instead appear on the surface [23,24]. The subsurface initiation makes it clear that the depth of the quenched layer and the hardness of the core of the base material are the two parameters to control to improve fatigue resistance.

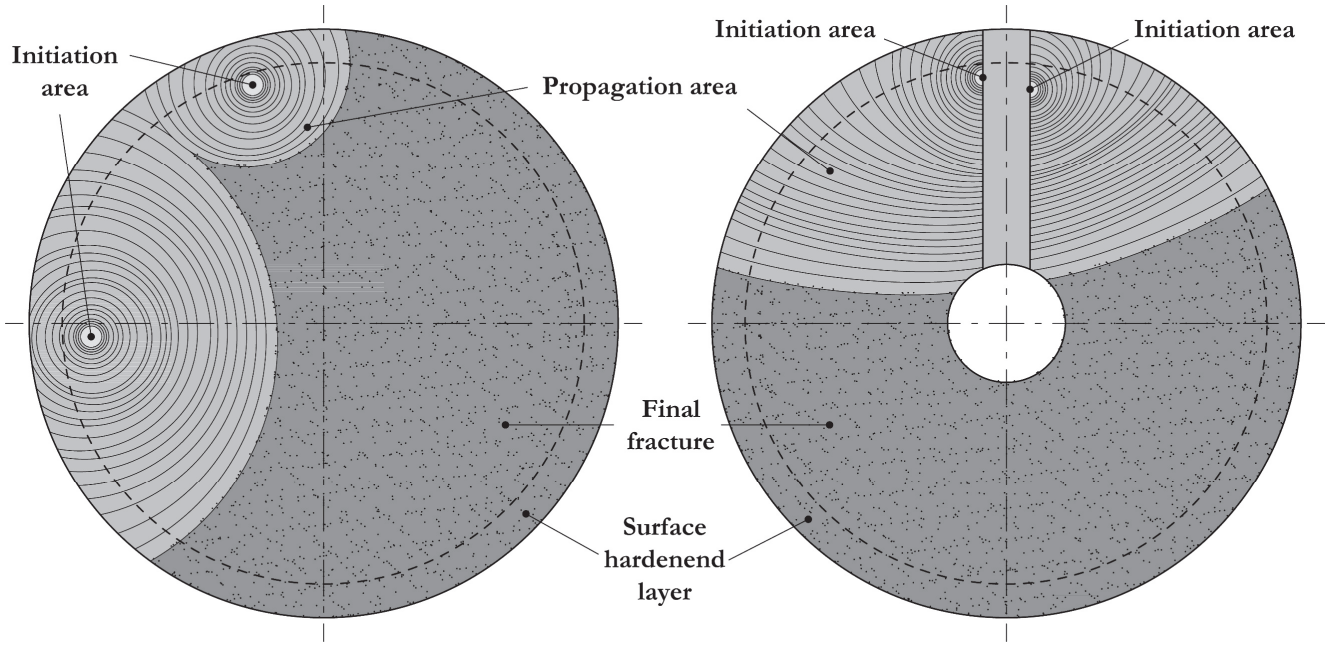


Figure 10: Schematic representation of the fatigue failure of two induction hardened steel shafts (left) C40 and (right) C50.

To evaluate the local fatigue strength of the surface-treated material, the aforementioned correlation between the ultimate tensile strength and the bending fatigue limit can be used [19] (valid only up to $\sigma_{FAb}$ = 700-750 MPa) or, more simply, the formulas proposed in the literature can be used [15].

Of particular interest is the simple and effective correlation proposed by Nakonieczny [15], independent of any residual stresses present, valid for rotating bending stresses (R = -1) in the range 340 < HV < 900:

$$\sigma_{FAb} = 1{,}98 HV_i - 0{,}0011 HV_i^2 \tag{4}$$

where $HV_i$ is the Vickers hardness measured where the local fatigue limit is to be determined. Fig. 11 shows the correlation between hardness and local bending fatigue limit.

### *Case hardening*

Case hardening is the most studied hardening heat treatment for fatigue resistance. Many studies have focused on gears, as case hardening is the most widely used surface treatment to harden gears, improving both the bending fatigue resistance of the tooth root and the contact fatigue resistance. In the case of case-hardened layers, the fatigue fracture mechanism is very different from that observed in components with hardened surfaces: failure always initiates from the external surface, whether smooth or notched, with localized semi-elliptical fracture of intergranular or mixed intergranular/transgranular type [25–27]. Fig. 12 shows the schematisation of an intergranular initiation with stable transgranular propagation, as observed in a case-hardened AISI/SAE 4320 steel (similar to 17NiCrMo6-4) [27].

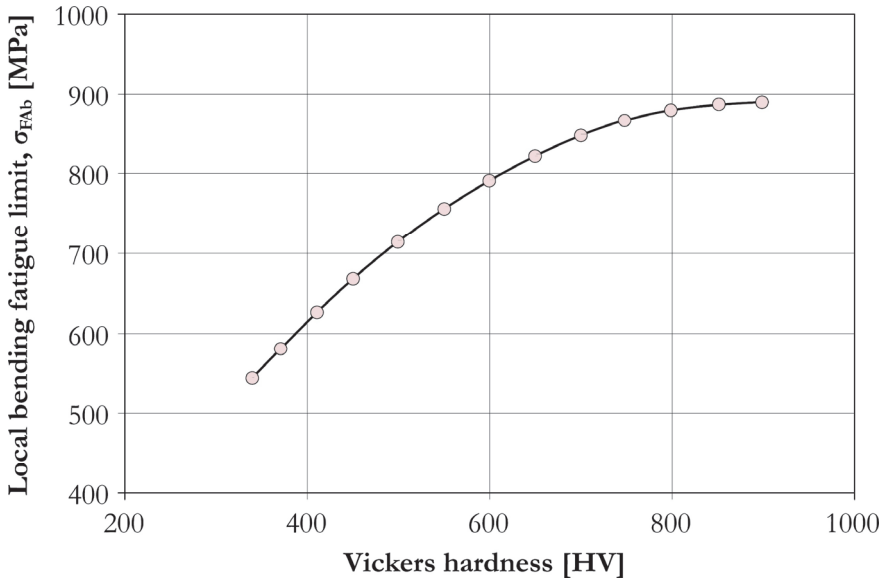


Figure 11: Correlation between local hardness and local bending fatigue limit for hardened surface layers estimated with (4).

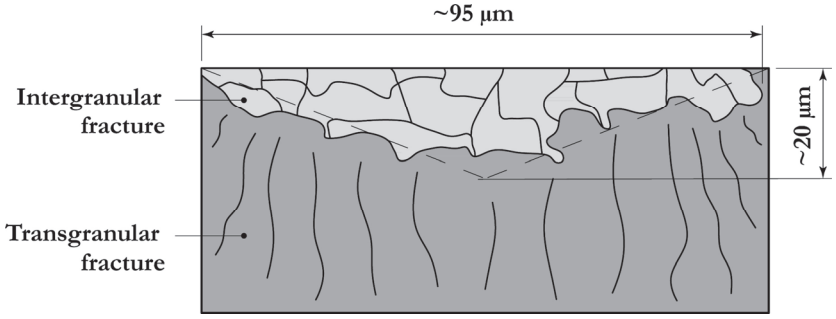


Figure 12: Schematisation of an intergranular initiation with subsequent stable transgranular propagation, as observed in a case-hardened AISI/SAE 4320 steel (similar to 17NiCrMo6-4). The defect is approximately √area = 40-45 µm.

The presence of a defect at the origin of fatigue failure also allows the calculation of the local fatigue limit using the approach proposed by Murakami [28,29] (which does not take into account any residual stresses). For the proposed example, the value of the defect propagation threshold is:

$$\Delta K_{th} = 0,0033\left(HV + 120\right)\left(\sqrt{area}\right)^{1/3} \cong 9 \div 9.5\, MPa\sqrt{m} \tag{5}$$

The surface hardness is approximately 680 HV [27].
The fatigue limit is:

$$\Delta\sigma_f = \frac{1.43\left(HV + 120\right)}{\left(\sqrt{area}\right)^{1/6}} \cong 605 \div 620\, MPa \tag{6}$$

to which any residual compressive stresses must be added.
From a metallurgical perspective, the main aspects related to the problem of carburised layer fatigue are listed below.

a. The typical failure of carburised layers, triggered by intergranular decohesion (Fig. 12), has been traced back to intergranular oxidation phenomena and the precipitation of phosphorus and/or cementite at grain boundaries [27,30–32]. Methods that can mitigate this problem (and consequently increase the material's fatigue strength) include:
   - reducing the average grain size of the base material,

- reducing the alloying elements that promote intergranular oxidation (particularly silicon and chromium),
- reducing the phosphorus content,
- reducing the average grain size after carburising: excellent results are obtained with a brief austenitising treatment (900°C x 30 min.) at the end of the carburising process and before stress relieving. This method is considered, by far, the most effective compared to the first three.

b. To improve fatigue strength, it is possible to act primarily on the compressive residual stresses of the carburised layer [26,27,33] that are related to the carbon content in the carburised layer. It is worth noting that carbon enrichment improves the hardness and strength of the carburised layer, but also promotes the formation of increasing amounts of retained austenite: high levels of retained austenite reduce compressive residual stresses after carburising. Consequently, the best bending fatigue properties are achieved with low carbon potentials in the carburising atmosphere (i.e., low carbon content at the surface of the carburised layer). This method maximises surface residual stresses and reduces the cementite precipitation at grain boundaries. Sub-zero cooling treatments do not appear to be beneficial for improving fatigue resistance: although the retained austenite content is reduced, no improvements in fatigue resistance are observed. The problem of deformation softening and redistribution of residual stresses due to cyclic stresses is present in carburised layers as well as in surface hardened ones.

c. Due to the particular initiation mode, the depth of the carburised layer does not have a great influence on the fatigue resistance of the sample/component: it has been observed that when the thickness of the carburised layer exceeds 10-15% of the diameter, no significant improvements in fatigue resistance are observed [34,35].

### *Nitriding*

Nitriding, the most recent surface hardening treatment, has become widespread on an industrial scale since the 1950s [36]. Widely used when high surface hardness and wear resistance of components are required, nitriding has recently also entered into competition with traditional hardening treatments for gears [37,38]. Regardless of the type of nitriding performed (gas, salt bath, ionic, etc.), an improvement in the fatigue life of the treated parts (high-cycle fatigue) is always observed: this increase is in the order of 13-105% on smooth specimens and 29-230% on notched specimens [17]. In general, similarly to what occurs on components with a hardened surface, fatigue failure initiation occurs beneath the nitrided layer in smooth components or those with limited notches (Fig. 13).

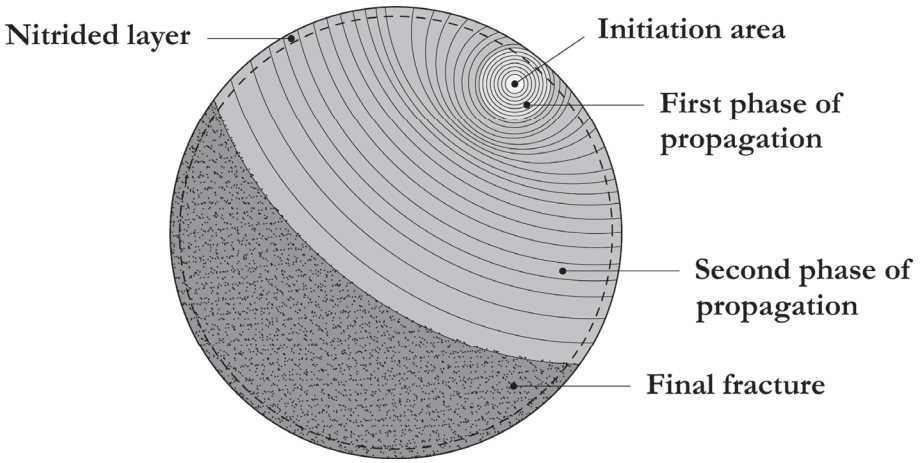


Figure 13: Schematic representation of the fatigue fracture surface of a nitrided specimen.

From a metallurgical point of view, the following problem of nitrided layer fatigue must be considered.

a. Nitriding generates significant compressive residual stresses on the surface of the parts (Fig. 14) independently from the process used [39,40]. The problem of deformation softening and redistribution of residual stresses due to cyclic stresses is lower compared to surface hardening and carburising treatments [41]. The cause lies in the different methods of forming the surface layer: in nitriding, hardening results from precipitation hardening phenomena, while in surface hardening and carburising, hardening is related to the interstitial solid solution of carbon in the iron lattice.

b. Although several authors have attempted to correlate surface hardness or hardening depth with the fatigue limit of nitrided steels, the results obtained are rather contradictory, and it seems that beyond a certain threshold (for both surface hardness and hardening depth) there is no effect on the improvement of fatigue resistance [42–44]. For high-cycle fatigue, even the thickness of the white layer (at least up to a maximum of 10 μm) does not appear to have any

effect on fatigue limit [44]. However, nitriding is known to improve the fatigue behaviour of notched specimens ($K_t$ > 1), rather than smooth specimens. Some authors report that the treatment can even eliminate the notch effect [45–47].

c. The core strength of the heat treated material is very important to ensure the optimal fatigue behaviour of nitrided components. Since fracture initiation occurs beneath the hardened layer, the mechanical properties of the steel core are often more important than the surface hardness of the nitrided layer. On smooth specimens (where fracture initiation certainly occurs beneath the nitrided layer), a correlation can be established between the fatigue limit of the base steel and that of its nitrided layer (Fig. 15).

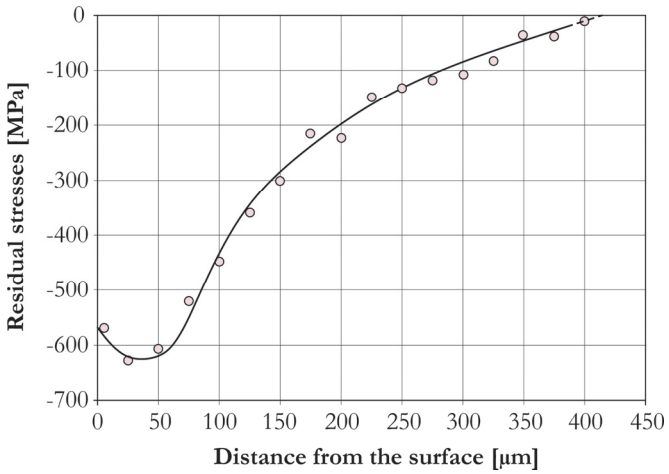


Figure 14: Residual stresses in a nitrided layer on EN 42CrMo4 (520 °C - 50 h), measured by X-ray diffraction [14].

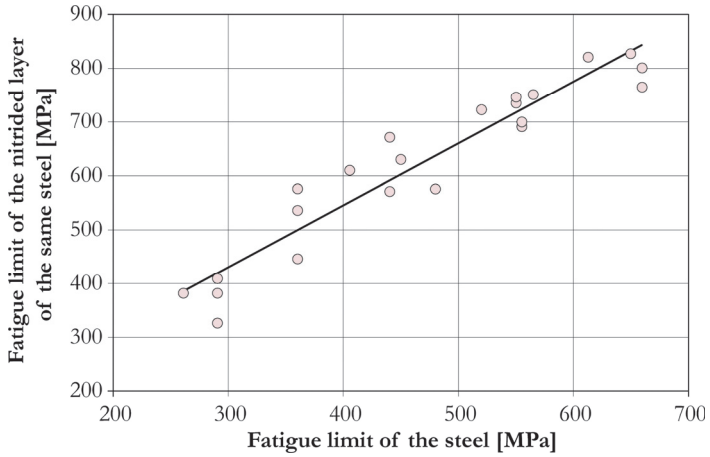


Figure 15: Fatigue limit of the base steel compared to the fatigue limit of the nitrided layer of the same steel. Rotating bending tests (R = -1) and specimens with $d$ = 5-10 mm (data taken from [15,16,36,43–46,48]).

For the evaluation of the local bending fatigue resistance of the nitrided layers ($\sigma_{FAb}$) we can refer to the correlation proposed by Nakonieczny [15] which, as already reported, is independent of any residual stresses (the formula is valid for rotating bending stresses R = -1 in the range 340 < HV < 900; for higher hardness values, consider 900HV).

## FATIGUE RESISTANCE EVALUATION MODEL OF A COMPONENT WITH HARDENED SURFACE

### *The failure condition*

The previous paragraphs allow to define three important parameters:

- the local bending fatigue strength ($\sigma_{FAb}$) at each point along the cross-section, that depends exclusively on the material strength after the heat treatment;
- the residual stress ($\sigma_{res}$) at each point along the cross-section, that depends on the type of hardening heat treatment;

- the external stress ($\sigma_{appl}$) at each point along the cross-section, that depends on the applied load condition (bending) and the shape of the component (smooth, $K_t = 1$ or notched, $K_t > 1$).

Therefore, the component will fail when, as the applied external stress increases, the local fatigue limit equals the sum of the external stress and the residual stress:

$$\sigma_{appl} + \sigma_{res} = \sigma_{FAb} \tag{7}$$

This method allows to evaluate both the stress that causes the failure of the surface-treated component and the point where the breakage will occur.

The local bending fatigue limit of the material can be estimated with (4) and then compared with a gradually increasing value of the effective stress obtained as the sum of the applied external stress ($\sigma_{appl}$) and the residual compressive stress ($\sigma_{res}$). The external stress is iteratively evaluated with (3) starting from a first tentative value of $\sigma_{o,sup}$ and then increasing it until the sum of $\sigma_{appl}$ and $\sigma_{res}$ (measured experimentally) is equal to the local bending fatigue limit. The intersection point indicates the depth at which failure will occur while the fatigue limit is instead equal to the value of the applied bending stress at the surface. To better clarify the method, three examples of practical application are presented below.

### *Applications of the method*

The first application example of the method [22] refers to quenched and tempered 50CrV4 steel (UTS = 1200 MPa, YS = 800 MPa, HV = 340); the material was induction hardened to a maximum hardness of 680 HV and a hardness effective depth of 0.7–0.8 mm. The fatigue test was performed on a Brugger-type specimen, subjected to three-point bending, with a cycle ratio R = 0.05.

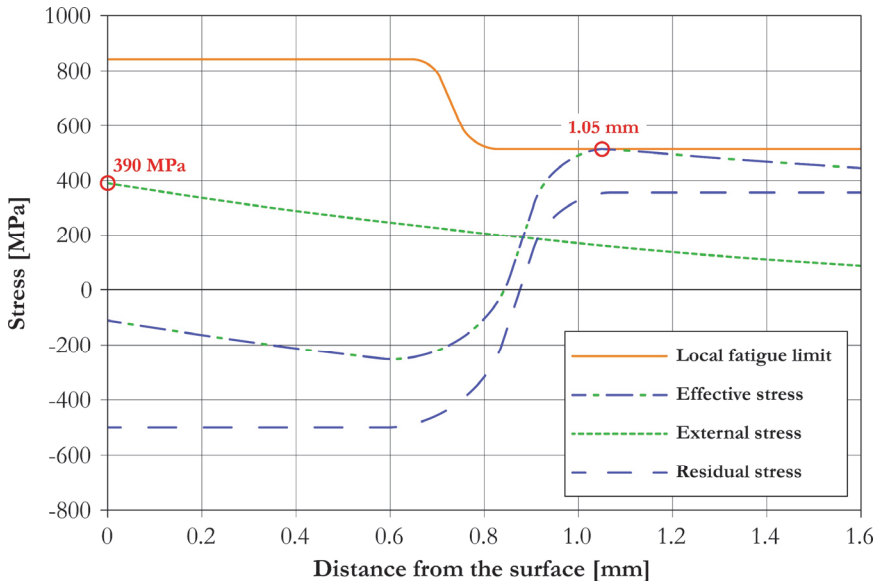


Figure 16: Simulation of local strength and stress state in an induction-hardened Brugger 50CrV4 steel specimen: estimation of the fatigue limit and fatigue crack initiation location.

The Brugger specimen has a specific geometry to represent the stress state at the root of the teeth of a gear wheel; the most stressed point of the specimen (where failure occurs) presents a change in cross-section with a theoretical notch effect equal to 1.56. Assuming a notch sensitivity $q = 0.925$, a $K_f$ coefficient of 1.518 is obtained.

The authors experimentally determined a fatigue limit of $\perp\sigma = 780 \pm 40$ MPa ($\sigma_a = 370$ MPa, $\sigma_m = 410$ MPa), with cracking initiated beneath the hardened layer. From these values, measured for R = 0.05, the fatigue limit at R = -1 can be derived using the well-known Gerber formula to account for the effect of mean stress [22]: ultimately, a fatigue limit of $\sigma_{FAb} = 420 \pm 25$ MPa ($K_t = 1.56$) is obtained. The rotating bending fatigue limit of the base material on smooth specimens ($\sigma_{FAb} = 507$ MPa) and the residual stress profile along the direction of maximum stress were also determined.

The simulation obtained with the proposed model is shown in Fig. 16. The local fatigue limit of the material was compared with a gradually increasing value of the applied external stress (appropriately corrected for the compressive residual stresses):

the estimated fatigue limit is equal to $\sigma_{FAb}$ = 390 MPa (the error, compared to the measured value, is approximately 7%); the predicted location of the initiation of fatigue crack is 1.05 mm from the component surface.

The second case study [49] involves cylindrical (hourglass-shaped) specimens made of case-hardened and tempered 16MnCr5 steel (core hardness HV = 300); a maximum hardness of 750 HV was achieved, an effective depth of 0.9 mm, and a total hardening depth of 1.5 mm. The fatigue test was performed in rotating bending with a cycle ratio R = -1. The hourglass specimen is used for rotating bending fatigue tests and to favour fracture initiation, it is not perfectly smooth but has a limited theoretical notch effect equal to 1.02. The article does not report the residual stress profile along the direction of maximum stress, but only the residual stress value measured at the surface (-120 MPa). The authors experimentally detect a fatigue limit of $\sigma_{FAb}$ = 750 ± 54 MPa.

The simulation obtained with the proposed model is shown in Fig. 17. The estimated fatigue limit is equal to $\sigma_{FAb}$ = 714 MPa (the error, compared to the measured value, is approximately 5%); the location of the initiation is predicted on the surface of the component.

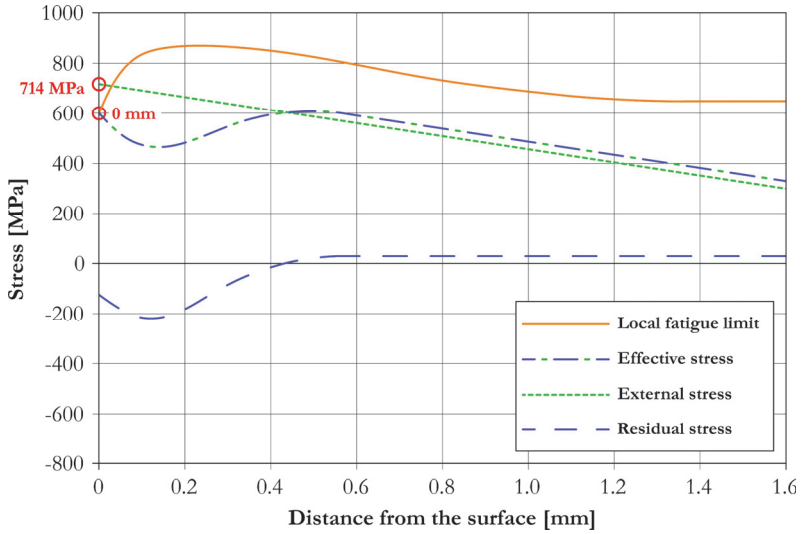


Figure 17: Simulation of local strength and stress state in a rotating bending specimen made of carburised 16MnCr5 steel: estimation of the fatigue limit and the fatigue crack initiation location.

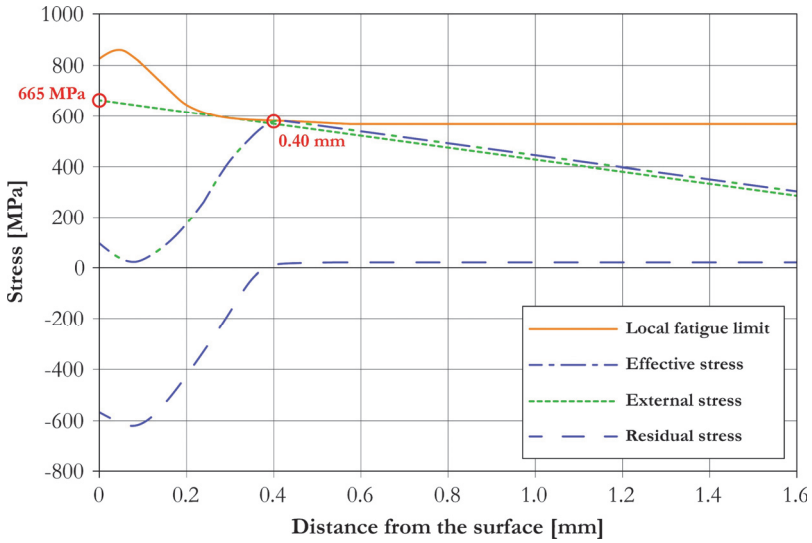


Figure 18: Simulation of local strength and stress state in a rotating bending specimen made of nitrided 42CrMo4 steel: estimation of the fatigue limit and the fatigue crack initiation location.

The third case study involves a surface nitriding treatment [15]. These are hourglass-shaped fatigue specimens ($K_t$ = 1.02) made of quenched and tempered 42CrMo4 steel (HV = 343). The steel was nitrided to a surface hardness of 715 HV; the maximum hardness is 826 HV, the effective depth is 0.2 mm, and the total depth is 0.3 mm. The fatigue test was performed

in rotating bending (R = -1). The article does not report the residual stress profile along the direction of maximum stress, but only the residual stress value measured at the surface (-600 MPa).

The authors experimentally detect a fatigue limit of $\sigma_{FAb}$ = 735 MPa (the standard deviation is not shown); fatigue initiation occurs 0.45 mm from the treated surface.

The simulation obtained with the proposed model is shown in Fig. 18. The fatigue limit estimate is $\sigma_{FAb}$ = 665 MPa (the error, compared to the measured value, is approximately 9%); the fatigue crack initiation point prediction is 0.4 mm from the component surface.

Tab. 2 summarises the results obtained in the three real-world experiments and the related estimates of the bending fatigue limit and the trigger position: the validity of the proposed method is underlined, with errors lower than 10% compared to the experimentally measured values.

| Steel grade | Heat treatment | $\sigma_{FAb}$ (R=-1) experimental [MPa] | $\sigma_{FAb}$ (R=-1) estimated [MPa] | Crack Initiation experimental [mm] | Crack Initiation estimated [mm] |
|---|---|---|---|---|---|
| 50CrV4 | Surface hardening | 420 | 390 (-7.1%) | > 0.80 | 1.05 |
| 16MnCr5 | Case Hardening | 750 | 714 (-4.8%) | Superficial | Superficial |
| 42CrMo4 | Nitriding | 735 | 665 (-9.4%) | 0.45 | 0.40 |

Table 2: Comparison between experimental data [15,22,49] and the estimation by the local fatigue limit method.

## CONCLUSIONS

This literature review systematically assessed the influence of the most common thermal and thermochemical surface hardening methods, specifically surface hardening, carburising, and nitriding, on the fatigue life of mechanical components. Given that fatigue remains the primary mechanism of structural failure in industrial applications, understanding the interaction between these treatments and cyclic loading is crucial. By synthesising the mechanical and metallurgical transformations induced by these processes, we presented a predictive model using the local fatigue limit approach. This model effectively integrates critical material variables to predict performance under bending stresses: (i) HV microhardness profiles, (ii) residual stress distributions, (iii) base material properties, and (iv) external stress states.

The validity of the proposed model was rigorously tested on three different cases: notched surface hardened specimen, smooth carburised specimen and smooth nitrided specimen. The high degree of correlation between model predictions and experimental results offers significant value for both academic and industrial applications. It provides a quantitative framework for identifying which metallurgical parameters should be optimised to maximise the service life. Ultimately, the application of the local fatigue limit approach has proven to be an accurate methodology for predicting the durability of superficial layers modified by surface hardening, carburising or nitriding.

This research facilitates the design strategy, allowing engineers to determine the most effective approach, such as optimizing the effective depth of the hardened layer or adjusting tempering parameters, to improve the fatigue behaviour of mechanical components even in case of high stress concentration.

## REFERENCES

[1] Casaroli, A., Scabini, E., Boniardi, M. V., Gerosa, R., Rivolta, B. (2026). Optimization of austenitic and ferritic steels for deep drawing. Part 1: metallurgical and mechanical analyses., Fracture and Structural Integrity, 20(75), pp. 104–123. DOI: https://doi.org/10.3221/IGF-ESIS.75.09.

[2] Casaroli, A., Scabini, E., Boniardi, M. V., Andreotti, R., Rivolta, B. (2026). Optimization of austenitic and ferritic steels for deep drawing. Part 2: FEM analyses with damage development, Fracture and Structural Integrity, 20(75), pp. 179–199. DOI: https://doi.org/10.3221/IGF-ESIS.75.13.

[3] Boniardi, M. V., Casaroli, A., Sirangelo, L., Monella, S., Mazzola, M. (2023). Failure analysis of boron steel components for automotive applications, Frattura Ed Integrita Strutturale, 17(64), pp. 137–147. DOI: https://doi.org/10.3221/IGF-ESIS.64.09.

[4] Bannantine, J.A., Comer, J.J., Handrock, J.L. (1990). Fundamentals of Metal Fatigue Analysis, Prentice Hall.

[5] D'Errico, F., Boniardi, M.V., Casaroli, A. (2012). Danneggiamento per pitting di acciai bonificati, cementati e nitrurati. La Metallurgia Italiana, 4, pp. 5-11.
[6] Casaroli, A., Boniardi, M., Conrado, E., Gorla, C., Crispino, C., Gerosa, R., Rivolta, B. (2024). Mechanical and metallurgical characterization of contact fatigue mechanisms in ADI spur gears, Eng. Fail. Anal., 165. DOI: https://doi.org/10.1016/j.engfailanal.2024.108775.
[7] Krauss, G. (1990). Steels: Heat Treatment and Processing Principles, ASM International.
[8] Boniardi, M., Guagliano, M., Casaroli, A., Andreotti, R., Ballerini, F. (2014). Large forgings: Microstructural evolution and residual stresses due to quenching treatments-a combined numerical and experimental approach, Mater. Perform. Charact., 3(4), pp. 118–136. DOI: https://doi.org/10.1520/MPC20130089.
[9] Thelning, K.-Erik. (1984). Steel and its heat treatment, Butterworths.
[10] ASM Internation. (1989). Carburizing: Processing and Performance, ASM International.
[11] Macherauch, E.., Hauk, V. (1987). Residual stresses in science and technology, DGM Informationsgesellschaft Verlag.
[12] Wulpi, D.J. (1999). Understanding How Components Fail, 3rd ed., ASM International.
[13] Juvinall, R.C., Marshek, K.M. (2021). Fundamentals of Machine Component Design, 7th ed., John Wiley & Sons.
[14] Boniardi, M. V., Casaroli, A. (2023). Metallurgia degli acciai - Parte seconda, Trafilix S.p.A.
[15] Nakonieczny, A. (2006). Fatigue Fracture of Nitrided and Carbonitrided Layers, Journal of Theoretical and Applied Mechanics, 44, pp. 713–730.
[16] Cazaud, R. (1953). Fatigue of Metals, Philosophical Library.
[17] Forrest, P.G. (1962). Fatigue of metals, Oxford, Pergamon Press, DOI: https://doi.org/10.1016/C2013-0-01695-7.
[18] Brooks, C.R., Choudhury, A. (1993). Metallurgical Failure Analysis, McGraw-Hill.
[19] Lee, Y.-Li., Pan, Jwo., Hathaway, Richard. (2011). Fatigue Testing and Analysis : Theory and Practice, Elsevier Science.
[20] Macherauch, E., Kloos, K.H. (1989). Bewertung von Eigenspannungen bei quasistatischer und schwingender Werkstoffbeanspruchung – Teil III, Materwiss. Werksttech., 20(3), pp. 82–91. DOI: https://doi.org/10.1002/mawe.19890200313.
[21] ASM International. (1991). ASM Handbook, Volume 04: Heat Treating.
[22] Bertini, L., Fontanari, V. (1999). Fatigue behaviour of induction hardened notched components, Int. J. Fatigue, 21, pp. 611–617. DOI: https://doi.org/10.1016/S0142-1123(99)00019-5.
[23] Mills, Kathleen. (1987). Metals Handbook: Fractography, ASM International.
[24] Palin-Luc, T., Coupard, D., Dumas, C., Bristiel, P. (2011). Simulation of multiaxial fatigue strength of steel component treated by surface induction hardening and comparison with experimental results, Int. J. Fatigue, 33(8), pp. 1040–1047. DOI: https://doi.org/10.1016/j.ijfatigue.2011.02.004.
[25] Wise, J.P., Krauss, G., Matlock, D.K. (2000). Microstructure and Fatigue Resistance of Carburized Steels, ASM International.
[26] Kim, D.-W., Lim, B.-S. (1999). Plasma and Vacuum Carburizing Processes and Mechanical Properties of SCM 415 Steel, vol. 13.
[27] Hyde, R.S., Cohen, R.E., Matlock, D.K., Krauss, G. (1992). Bending Fatigue Crack Characterization and Fracture Toughness of Gas Carburized SAE 4320 Steel.
[28] Yukitaka, M., Masahiro, E. (1983). Quantitative evaluation of fatigue strength of metals containing various small defects or cracks, Eng. Fract. Mech., 17(1), pp. 1–15. DOI: https://doi.org/10.1016/0013-7944(83)90018-8.
[29] Murakami, Y., Endo, M. (1994). Effects of defects, inclusions and inhomogeneities on fatigue strength, Int. J. Fatigue, 16(3), pp. 163–182. DOI: https://doi.org/10.1016/0142-1123(94)90001-9.
[30] Cavallaro, G.P., Wilks, T.P., Subramanian, C., Stratford, K.N., French, P., Allison, J.E. (1995). Bending fatigue and contact fatigue characteristics of carburized gears, 71, DOI: https://doi.org/10.1016/0257-8972(94)01019-F.
[31] Hyde, R.S., Krauss, G., Matlock, D.K. (1994). The Effect of Reheat Treatments on Fatigue and Fracture of Carburized Steels.
[32] Pacheco, J.L., Krauss, G. (1989). Microstructure and High Bending Fatigue Strength in Carburized Steel, Journal of Heat Treating, 7, pp. 77-86.
[33] Krug, T., Lang, K.H., Fett, T., Löhe, D. (2007). Influence of residual stresses and mean load on the fatigue strength of case-hardened notched specimens, Materials Science and Engineering: A, 468–470, pp. 158–163. DOI: https://doi.org/10.1016/j.msea.2006.07.167.
[34] Genel, K., Demirkol, M. (1999). Effect of case depth on fatigue performance of AISI 8620 carburized steel, Int. J. Fatigue, 21, pp. 207–212. DOI: https://doi.org/10.1016/S0142-1123(98)00061-9.
[35] Dawes, C., Cooksey, R.J. (1966). Surface Treatment of Engineering Components, Heat Treatment of Metals, Special Report No. 95.

[36] Pye, D. (2003). Practical Nitriding and Ferritic Nitrocarburizing. ASM International.
[37] Boniardi, M., D'Errico, F., Tagliabue, C. (2006). Influence of carburizing and nitriding on failure of gears - A case study, Eng. Fail. Anal., 13(3), pp. 312–339. DOI: https://doi.org/10.1016/j.engfailanal.2005.02.021.
[38] Natarajan, R., Krishnamurthy, R. (1984). Fatigue Performance of Surface Treated Gears., Proceedings of the 2nd International Conference on Fatigue and Fatigue Thresholds (Fatigue 84), Engineering Materials Advisory Services (EMAS).
[39] Mittemeijer, E.J. (1983). The Relation between Residual Macro- and Microstresses and Mechanical Properties of Case Hardened Steels., Proceedings of the 112th AIME Annual Symposium (Case Hardened Steels: Microstructure and Properties), The Metallurgical Society of AIME.
[40] Lieurade, H.P. (1988). Effet des Contraintes Résiduelles sur le Comportement à la Fatigue des Pièces et des Structures Industrielles, Traitement Thermique.
[41] Ali Terres, M. (2003). Tenue en fatigue flexion d'un acier nitruré, Annales de Chimie Science Des Matériaux, 28(1), pp. 25–41. DOI: https://doi.org/10.1016/S0151-9107(03)00003-5.
[42] Cowling, J.M., Martin, J.W. (1979). Effect of Internal Residual Stresses on the Fatigue Behaviour of Nitrided En41B Steel., Proceedings of the International Conference on Heat Treatment (Heat Treatment '79), The Metals Society.
[43] Braam, J.J., Gommers, A.W.J., Van Der Zwaag, S. (1997). The influence of the nitriding temperature on the fatigue limit of 42CrMo4 and En40B steel, J. Mater. Sci. Lett., 16(16), pp. 1327–1329. DOI: https://doi.org/10.1023/A:1018507915634.
[44] Terent'ev, V.F., Michugina, M.S., Kolmakov, A.G., Kvedaras, V., Čiuplys, V., Čiuplys, A., Vilys, J., Baikov, A.A. (2007). The effect of nitriding on fatigue strength of structural alloys, Mechanika. DOI: https://doi.org/10.5755/j02.mech.14797.
[45] Hrubý, V., Holemár, A. (1981). Influence of Ion Nitriding on Fatigue Characteristic Changes of ČSN 16420.6 Steel, Strojírenská Výroba.
[46] Kawagoishi, N., Morino, K., Oka, T., Tanaka, N., Fukada, K. (2000). Fatigue Strength of Radical Nitrided Bearing Steel., Transaction of the Japan Society of Mechanical Engineers, Series A, 66(651), pp. 2036–2043. DOI: https://doi.org/10.1299/kikaia.66.2036.
[47] Gligorijević, R., Jevtić, J., Borak, D. (n.d.). Combination of shot-peened and gas nitrided for fatigue improvement of nodular iron connecting rods.
[48] Guechichi, H., Castex, L. (2006). Fatigue limits prediction of surface treated materials, J. Mater. Process. Technol., 172(3), pp. 381–387. DOI: https://doi.org/10.1016/j.jmatprotec.2005.10.010.
[49] La Vecchia, G.M., Lecis, N., Troglio, S. (2006). Interventi funzionali dedicati alla modifica della superficie degli ingranaggi: la cementazione e la nitrurazione come pretrattamento di rivestimenti PVD, La Metallurgia Italiana, 4.